STRATOSPHERIC MEMORY: EFFECTS ON THE TROPOSPHERE

Mark P. Baldwin*, David B. Stephenson, David W.J. Thompson,
Timothy J. Dunkerton, Andrew J. Charlton, Alan O'Neill

We use an empirical statistical model to demonstrate significant skill in extended-range forecasts of the monthly-mean Arctic Oscillation (AO). Forecast skill derives from long-lived circulation anomalies in the lowermost stratosphere and is greatest during boreal winter. A comparison to the Southern Hemisphere provides evidence that both the timescale and predictability of the AO depend on the presence of long-lived circulation anomalies just above the tropopause. These circulation anomalies most likely affect the troposphere through changes to waves in the upper troposphere, which induce surface pressure changes corresponding to the AO.

1. INTRODUCTION

Deterministic prediction of daily weather, using numerical forecast models, is limited to several days. As the lead-time increases to a week and beyond, deterministic prediction of the weather for a particular day gives way to stochastic prediction of the time-averaged weather, which is more predictable than its instantaneous state (*WMO,* 2001). Weather forecasts beyond 10 days are called "extended-range" predictions**; they may be ensemble forecasts, in which many model forecasts with slightly differing initial conditions are averaged together, or they may be based on empirical statistical models trained on historical data.

Forecast skill in predicting the time-averaged state of the atmosphere beyond 10 days comes mainly from slow and predictable influences of Earth's surface. In the Northern Hemisphere extratropics, the main contributor to predictability is tropical sea surface temperature anomalies (*Kanamitsu et al.,* 2002*; Hoerling and Kumar,* 2003), with possible contributions from soil moisture, vegetation, snow and ice cover, land surface temperature and albedo, and sea ice movement and extent. Forecast skill also derives from memory within the atmosphere, or phenomenon with long lifetimes, such as the Madden-Julian Oscillation in the tropical troposphere (*Madden and Julian, 1971*). There is growing evidence that additional extended-range tropospheric forecast skill may also come from slow variations of the circulation of the stratosphere (*Baldwin and Dunkerton,* 1999; 2001*; Thompson et al.,* 2002).

In general, the largest spatial scales of atmospheric variability are more persistent and easier to forecast than the smaller scales. The Arctic Oscillation (AO) (*Thompson and Wallace,* 1998), similar to the North Atlantic Oscillation (*Hurrell,* 1995*; Wallace,* 2000*),* is a planetary-scale pattern of near-surface (1000 hPa) variability characterized by movement of atmospheric mass between high and low latitudes and a corresponding out-of-phase relation, or dipole, in the strength of the zonal flow along ~55°N and ~35°N. The AO exerts a strong influence on wintertime climate throughout middle and high-latitude continental regions. It affects not only average conditions, but also the day-to-day variability, modulating rainfall and storm tracks, the frequency of occurrence of high-latitude blocking events, and cold air outbreaks (*Thompson and Wallace, 2001*).

The Northern Annular Mode (NAM) is identical to the AO at 1000 hPa, but we define it separately at each isobaric level from Earth's surface through the stratosphere. The NAM is defined as the leading empirical orthogonal function (EOF) of slowly varying (e.g., month-to-month) wintertime hemispheric geopotential at each level, and is the spatial pattern that accounts for the greatest fraction of geopotential variance. Daily indices of the annular modes are calculated for each level by projecting daily geopotential anomalies onto the leading EOF patterns. For details of the calculation see *Baldwin and Dunkerton* (2001). Time-height analysis of the NAM links variations in the strength of the stratospheric polar vortex downward to the AO. We use National Centers for Environmental Prediction (NCEP) reanalysis data for 1000–10 hPa during 1958–2002. Stratospheric NAM variations, which are driven mainly by upward-propagating planetary-scale waves of tropospheric origin, tend to descend through the stratosphere and create long-lived NAM anomalies just above the tropopause. On average lower stratospheric NAM anomalies are followed by long-lived AO anomalies of the same sign (*Baldwin and Dunkerton, 1999; 2001*). This observation suggests that the timescale of the NAM may be a key to understanding how stratospheric circulation anomalies affect the troposphere.

2. NAM TIMESCALE

We define the timescale of NAM anomalies as the time for the autocorrelation function of the NAM to decrease to 1/*e*, (~0.368, the "*e*-folding time"). Based on data from 1958 to 2002, we find that the timescale of the NAM in the stratosphere is greater than that in the troposphere during all seasons (Fig. 1a).

---

*Corresponding author address: Mark P. Baldwin, NorthWest Research Associates, PO Box 3027, Bellevue, WA, 98007 USA, Phone: 425-644-9660, ext. 323, e-mail: mark@nwra.com

**World Meteorological Organization, World Weather Watch, Appendix I.4 to the Manual on Global data Processing Systems.

During winter the longest NAM timescale occurs just above the tropopause, consistent with the radiative timescale (*Shine, 1987*). The timescale of the AO is greatest during winter.

We hypothesize that during winter the timescale of the AO is enhanced by persistent NAM anomalies in the lowermost stratosphere. By itself the coincidence of the tropospheric and stratospheric maxima (Fig 1a) is merely suggestive of a stratosphere-troposphere coupling. For evidence in support of the hypothesis that stratospheric NAM anomalies increase the timescale of the AO, we examine the timescale of the Southern Annular Mode. For the Southern Hemisphere we used NCEP data from 1979–2001. Stratospheric data prior to 1979 are considered unreliable, and we did not use the highly unusual winter-spring events of 2002, which included the only observed major stratospheric warming in the Southern Hemisphere. In the troposphere the timescale of the SAM has a peak during late spring (November–December) superposed on a gentle annual cycle that is maximizes during winter (Fig. 1b). The late spring maximum in the timescale of the tropospheric SAM coincides with the largest SAM anomalies just above the tropopause (Fig. 1c). Climatologically, the Southern Hemisphere stratospheric polar vortex is strong throughout the winter, with relatively small SAM anomalies. It is not until spring, when the vortex begins to diminish, that wave, mean-flow interaction results in large SAM anomalies (*Thompson and Wallace,* 2000). The Southern Hemisphere vortex breaks down first in the upper stratosphere, and progresses downward. This process is reflected in the time-height development of the SAM variance; the maximum in SAM variance progresses downward during spring, peaking during November–December just above the tropopause. The maximum timescale of the tropospheric SAM (Fig. 1b) aligns precisely with the maximum SAM variance just above the tropopause (Fig. 1c). In both hemispheres the timescale of the tropospheric annular mode is a maximum when the amplitude of lower stratospheric annular mode anomalies are largest. The longer timescale of the AO during winter is also consistent with general circulation model experiments in which the timescale of the AO is found to decrease when stratospheric variability is artificially suppressed (*Norton,* 2003).

3. AO FORECASTS

The observation that long-lived AO anomalies tend to follow stratospheric NAM anomalies of the same sign suggests the use of a prediction model in which the NAM at one or more level is used to predict the time-averaged value of the AO. Data analysis (*Charlton et al.,* 2003) suggests that there is a linear relationship between the AO and subsequent NAM anomalies in the lower stratosphere, so that a linear statistical model appears to be an appropriate first way to investigate the relationship between stratospheric NAM values and future values of the AO. We demonstrate this technique by predicting the monthly mean AO, but we begin the forecast period after 10 days in order to exclude the initial time period when numerical forecasts of daily weather have appreciable skill. Our linear prediction model uses the present value of the NAM at one level between 1000 and 10 hPa to predict the monthly-mean AO beginning 10 days later:

$$\overline{A}(t+L) = \beta_0 + \beta_1 N(t) + \varepsilon$$

where A represents the AO, L=10+(30/2)=25 days, $\overline{A}(t+L)$ represents the one-month mean of the AO centered on time $t+L$ (starting at time $t+L$-15 and continuing to time $t+L+$15), $N(t)$ represents the NAM at one level at time t; β_0 and β_1 are regression parameters to be estimated and ε represents noise.

We performed least-squares regressions to calculate the percent variance of $\overline{A}(t+L)$ that is accounted for by the predictor series $N(t)$, as a function of height and time of year (Fig. 2a). Predictability of the AO is greatest during the extended winter season (October–April). The stratospheric NAM is a better predictor of the AO than the AO is of itself—and it does so for a longer season (Fig. 2b). The optimum single level for forecasting the AO is 150 hPa (~13 km), which is the lowest data level that lies entirely above the tropopause in the extratropics.

In order to test predictability of the AO it is necessary to make forecasts and assess their skill. Using all years of December–February data the NAM at 150 hPa accounts for 20.2% of the variance of the AO 10–40 days later. In order to avoid artificial skill we performed cross-validated forecasts by removing one winter at a time, estimating β_0 and β_1, and then forecasting the missing winter. The cross-validated skill dropped slightly to 17.9%. If instead of the 150-hPa NAM, the AO is used to predict itself, the cross-validated skill is 12.3%. We also tried forecasts using both the 150-hPA NAM and the AO together, but we obtained an identical cross-validated skill of 17.9%, indicating that the AO adds no information that is not already in the 150-hPa NAM, and that the 150-hPa NAM is a sufficient predictor.

4. OPTIMAL PATTERNS

Our prediction methodology uses annular mode indices as both predictors and predictands, so the results thus far have demonstrated only that the forecasting relationship projects onto the annular mode patterns. There is no reason to believe a priori that the annular mode patterns optimize the relationship between circulation anomalies in the lowermost stratosphere and subsequent 1000-hPa anomalies. We used Maximum Covariance Analysis (MCA), which maximizes the covariance between any two fields (also know as Singular Value Decomposition analysis), to pair daily 150-hPa geopotential fields with monthly-mean1000-hPa fields beginning 10 days later. We found that the beginning 10 days later. We found that the MCA patterns for 1000 and 150 hPa were nearly identical to the AO and 150-hPa NAM patterns, respectively (Fig. 3). Although we are not aware of any theoretical reason to expect this result, the optimal spatial patterns for both the predictor and predictand are nearly identical to the annular mode patterns.

5. WAVE INTERACTIONS

The interaction between NAM anomalies just above the tropopause (~150 hPa) and waves in the upper troposphere (~300 hPa) may be the primary mechanism by which stratospheric anomalies induce changes to the troposphere (*Shepherd,* 2002). Both synoptic-scale and planetary-scale waves penetrate the lowermost stratosphere, providing a region of overlap between the NAM anomalies and the waves. Based on the observations (Figs. 1–3), we reason that the 150-hPa NAM (or some similar quantity involving zonal-mean wind) must be involved in coupling to the troposphere.

Previous work has shown that the tropospheric NAM is driven by transient momentum flux anomalies (*Limpasuvan and Hartmann,* 2002). These anomalies tend to occur over a broad latitudinal band, peaking in midlatitudes, so that the momentum flux convergence anomalies form a north-south dipole, forcing both the NAM and a dipole in zonal-mean wind. Theoretically, the response to any such forcing is both a zonal wind acceleration and a mass redistribution (changes to surface pressure) as part of an induced circulation in the meridional plane (*Haynes and Shepherd,* 1989). Through this mechanism upper tropospheric momentum flux anomalies lead directly to AO changes. During December–February the daily correlation between 300-hPa momentum flux anomalies (latitudinally-averaged north of 20°N) and the rate of change of the AO index is 0.46.

For specific evidence that lower stratospheric NAM anomalies affect momentum fluxes in the upper troposphere we examined how the 150-hPa NAM affects correlations between 300-hPa eddy momentum fluxes and the 300-hPa NAM. *Lorenz and Hartmann* (2003) found similar lag correlations between the leading EOF of 1000–100-hPa zonal wind and eddy momentum flux convergences. We categorized each day during December–February by whether or not the NAM anomalies increased in magnitude between 300 and 150 hPa. On 38% (1575) of the days the NAM anomaly strengthened with height (had the same sign anomaly at both levels and was numerically larger at 150 hPa). We compared the distributions of the 300-hPa NAM for the two categories and found that neither the standard deviation nor the mean differed significantly from that for all days. When the NAM strengthened with height the mean was 0.028 and the standard deviation was 0.90. When the NAM weakened with height the mean was -.018 and the standard deviation was 1.06.

When the NAM strengthened with height upper tropospheric momentum flux anomalies were more effective at forcing upper tropospheric NAM anomalies of the same sign, and they did so for a longer time (Fig. 4a). When the NAM weakened with height the lag correlations were smaller and dropped to near zero within a few days. This difference supports of the hypothesis that the lower stratospheric NAM modulates momentum fluxes in the upper troposphere.

We find that both planetary-scale waves and synoptic-scale waves are involved. The propagation of planetary waves is particularly sensitive to wind anomalies just above the tropopause (*Chen and Robinson*, 1992), but planetary waves 1–2 account for only ~25% of the variance of the momentum flux at 300 hPa. When the NAM strengthened with height momentum fluxes from planetary waves 1–2 had a greater effect on the NAM, especially at positive lags (Fig 4b); when waves 3 and higher were used (Fig. 4c), the effect was similar to that for all waves (Fig 4a). These results provide evidence that both planetary-scale and synoptic-scale tropospheric waves are affected by stratospheric NAM anomalies.

The wave coupling mechanism does not preclude other ways in which the stratosphere could affect the troposphere, such as "downward control" (*Haynes et al.,* 1991), which relates steady-state wave drag to vertical mass flow (and by continuity, surface pressure changes), or planetary wave reflection (*Perlwitz and Graf,* 2001*; Perlwitz and Harnik,* 2003). The wave coupling mechanism is also consistent with studies of potential vorticity "inversion" in which lower stratospheric circulation anomalies induce AO-like changes to surface pressure of realistic magnitudes (*Black,* 2002).

6. SUMMARY

Our results have implications for numerical extended-range weather forecasting. Forecast models that do not adequately resolve the stratosphere (or that do not have realistic NAM anomalies in the lowermost stratosphere) will likely not be able to simulate the additional predictive skill from the stratospheric memory effect. A complete understanding of the details of the mechanism by which the lower stratospheric NAM affects waves in the upper troposphere will likely require carefully designed numerical experiments. On longer timescales, the wave coupling mechanism would presumably allow stratospheric signals (e.g., greenhouse gas and ozone changes, solar/UV variations, and the quasi-biennial oscillation) to affect surface climate, and for trends in the stratospheric NAM to be reflected in the AO index.

Acknowledgements: We thank T.G. Shepherd, P.H. Haynes, and D.A. Orland for discussions. The NCEP reanalysis data were obtained from the NOAA-CIRES Climate Diagnostics Center.

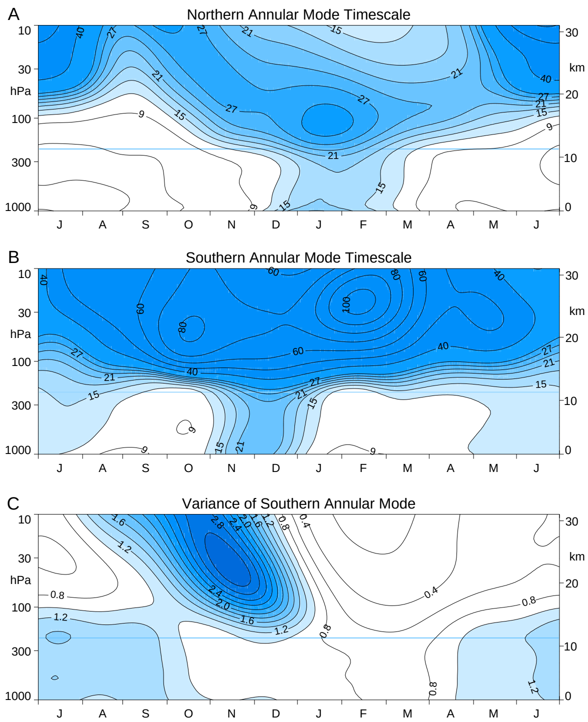

Fig. 1. **(A)** Timescale of the Northern Annular Mode as measured by the time (days) for the autocorrelation function to drop to 1/*e* (~0.378). The horizontal line in each panel represents the approximate tropopause. Daily values are a time average using Gaussian weighting with a full width at half maximum (FWHM) of 60 days (σ=26 days). The timescale is estimated with a least-squares fit of an exponential curve to the autocorrelation function. The contour interval is three days up to 30 days, and 10 days at higher values. **(B)** As in **(A)**, except Southern Annular Mode. **(C)** Variance or the Southern Annular Mode. Daily values were obtained using the same methodology as **(A)**. SAM time series at each level are normalized to unit standard deviation.

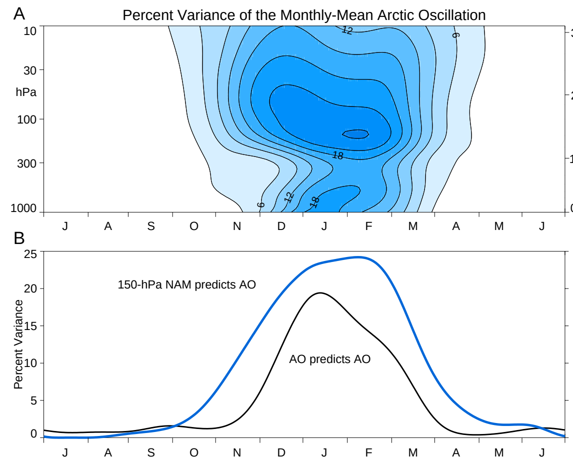

Fig. 2. **(A)** Predictability of the monthly-mean Arctic Oscillation after a 10-day lead. Values are obtained by linear regression between the daily NAM time series and the monthly-mean Arctic Oscillation beginning after 10 days, and are displayed as percent variance of the monthly-mean Arctic Oscillation, with darker shading indicating greater predictability. Daily values represent an average using Gaussian weighting with FWHM=60 days. **(B)** Cross sections through **(A)** at 1000 and 150 hPa. upper curve: 150-hPa NAM predicts the monthly-mean AO; lower curve: AO predicts the monthly-mean AO.

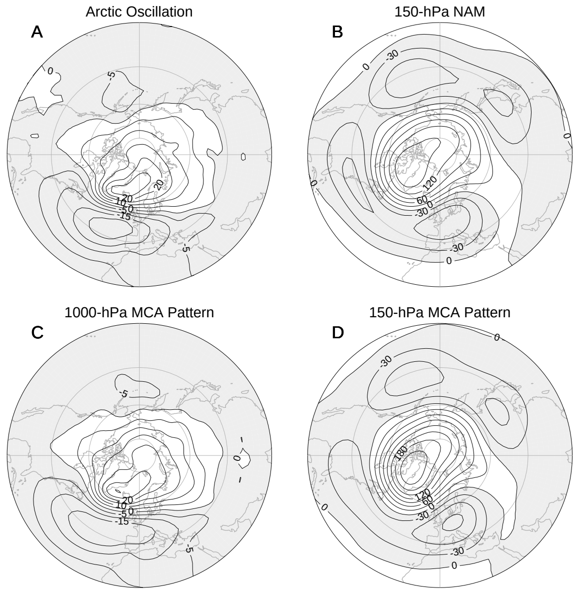

Fig. 3. **(A)** Arctic Oscillation regression pattern (geopotential meters) obtained as the leading empirical orthogonal function (EOF) of monthly-mean December–February 1000-hPa geopotential poleward of 20°N. **(B)** 150-hPa NAM; as in **(A)** except using 150-hPa geopotential. **(C)** and **(D)** Leading Maximum Covariance Analysis patterns between geopotential at 150 and monthly-mean 1000 hPa geopotential beginning 10 days later. For comparison with the EOF patterns, **(C)** is normalized to have the same area-weighted spatial variance as **(A)**, and **(D)** is normalized to have the same area-weighted spatial variance as **(B)**. The area-weighted spatial correlation is 0.95 between **(A)** and **(C)**, and 0.96 between **(B)** and **(D)**.

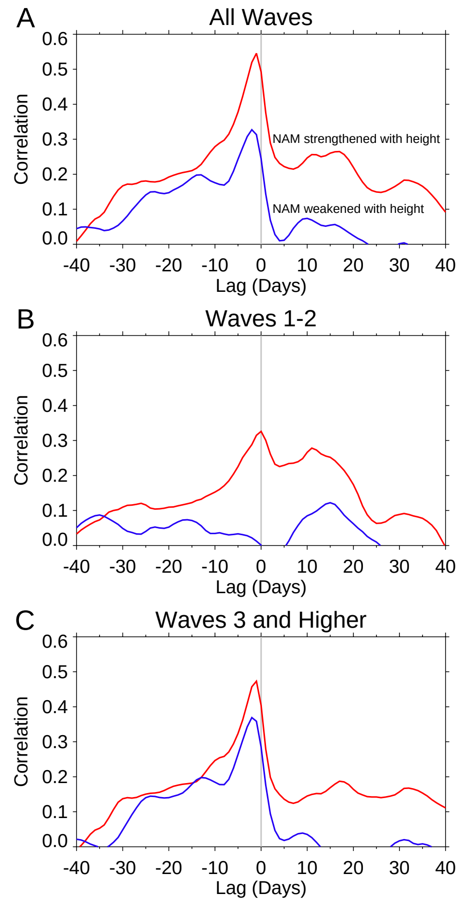

Fig. 4. Cross correlation between 300-hPa NAM and 300-hPa zonally-averaged momentum flux poleward of 20°N, during December–February. Negative lag means that the momentum flux anomalies lead the annular mode anomalies. (**A**) All waves. The upper curve is for the subset of days on which the 150-hPa NAM was stronger than the 300-hPa NAM. The lower curve is for the subset of days on which the 150-hPa NAM was weaker than the 300-hPa NAM. (**B**) As in (**A**), except waves 1–2. (**C**) As in (**A**), except waves 3 and higher.

7. REFERENCES

Baldwin, M.P., T.J. Dunkerton, *J. Geophys. Res*. **104**, 30937 (1999).

Baldwin, M.P., T.J. Dunkerton, *Science* **294**, 581 (2001).

Black, R.X., *J. Climate*, **15**, 268 (2002).

Charlton, A.J., A. O'Neill, D.B. Stephenson, W.A. Lahoz, M.P. Baldwin, *Q. J. R. Meteor. Soc*., submitted, 2003.

Chen, P., W.A. Robinson, *J. Atmos. Sci*. **49**, 2533 (1992).

Haynes, P.H., T.G. Shepherd, *Q. J. R. Meteorol. Soc*. **115**, 1181 (1989).

Haynes, P.H., C.J. Marks, M.E. McIntyre, T.G. Shepherd, K.P. Shine, *J. Atmos. Sci*. **48**, 651 (1991).

Hoerling, M., A. Kumar, *Science* **299**, 691 (2003).

Hurrell, J.W., *Science* **269**, 676 (1995).

Kanamitsu, M. *et al.*, *Bull. Am. Meteor. Soc*. **83**, 1019 (2002).

Limpasuvan, V., D.H. Hartmann, *J. Climate* **13**, 4414 (2000).

Lorenz, D., D.H. Hartmann, *J. Climate*, accepted, 2003

Madden, R.A., Julian, P.R., *J. Atmos. Sci*. **28**, 702 (1971).

Norton, W.A., *Geophys. Res. Lett*., submitted, 2003.

Perlwitz, J., H.-F. Graf, *Geophys. Res. Lett*. **28**, 271 (2001).

Perlwitz, J., N. Harnik, *J. Climate*, submitted, 2003.

Shepherd, T.G., *J. Meteorol. Soc. Japan* **80**, 769 (2002).

Thompson, D.W.J., M.P. Baldwin, J.M. Wallace, *J. Climate* **15**, 1421 (2002).

Thompson, D.W.J., J.M. Wallace, *Geophys. Res. Lett*. **25**, 1297 (1998).

Thompson, D.W.J., J.M. Wallace, *J. Climate* **13**, 1000 (2000).

Thompson, D.W.J., J.M. Wallace, *Science* **293**, 85 (2001).

Wallace, J.M., *Quart. J. Royal. Met. Soc*. **126**, 791 (2000).

World Meteorological Organization, Commission for Basic Systems, Expert Team Meeting on Infrastructure for Long-Range Forecasting, Geneva, Switzerland, 12–16 November 2001 (CBS ET/ILRF/Doc.3).